27. K. D. Dorkenoo, P. H. Pfromm, *Macromolecules* **33**, 3747 (2000).
28. B. W. Rowe, L. M. Robeson, B. D. Freeman, D. R. Paul, *J. Membr. Sci.* **360**, 58 (2010).
29. H. B. Park *et al.*, *Science* **318**, 254 (2007).
30. N. Du *et al.*, *Nat. Mater.* **10**, 372 (2011).
31. N. Y. Du, G. P. Robertson, I. Pinnau, M. D. Guiver, *Macromolecules* **43**, 8580 (2010).
32. N. Y. Du, G. P. Robertson, J. S. Song, I. Pinnau, M. D. Guiver, *Macromolecules* **42**, 6038 (2009).
33. N. Y. Du, G. P. Robertson, I. Pinnau, M. D. Guiver, *Macromolecules* **42**, 6023 (2009).
34. N. Du, G. P. Robertson, I. Pinnau, S. Thomas, M. D. Guiver, *Macromol. Rapid Commun.* **30**, 584 (2009).
35. N. Y. Du *et al.*, *Macromolecules* **41**, 9656 (2008).
36. R. Short *et al.*, *Chem. Commun. (Camb.)* **47**, 6822 (2011).
37. D. Fritsch, G. Bengtson, M. Carta, N. B. McKeown, *Macromol. Chem. Phys.* **212**, 1137 (2011).
38. B. S. Ghanem, N. B. McKeown, P. M. Budd, D. Fritsch, *Macromolecules* **41**, 1640 (2008).
39. B. S. Ghanem *et al.*, *Macromolecules* **42**, 7881 (2009).
40. M. Gringolts *et al.*, *Macromolecules* **43**, 7165 (2010).
41. M. Calle, A. E. Lozano, J. G. de La Campa, J. de Abajo, *Macromolecules* **43**, 2268 (2010).
42. Y. Hu, M. Shiotsuki, F. Sanda, B. D. Freeman, T. Masuda, *Macromolecules* **41**, 8525 (2008).

Acknowledgments: Part of the work leading to these results has received funding from the European Community's Seventh Framework Programme (FP7/2007-2013) under grant agreement NMP3-SL-2009-228631, project DoubleNanoMem. We also thank the Engineering and Physical Sciences Research Council for funding (grants EP/G01244X and EP/G062129/1). K. Pilnácek and G. Clarizia are gratefully acknowledged for their help in the data elaboration and the performance of mixed-gas permeation measurements. We thank G. Hutchings (Cardiff University) for reading the manuscript and making helpful suggestions. A patent has been filed through Cardiff University on the polymer synthesis presented in this report (UK patent application PCT/GB2011/051703; WO 2012/035327 (2010).

Supplementary Materials

www.sciencemag.org/cgi/content/full/339/6117/303/DC1
Materials and Methods
Figs. S1 to S5
Table S1
References (*43*–*51*)

27 July 2012; accepted 6 November 2012
10.1126/science.1228032

Olefin Cyclopropanation via Carbene Transfer Catalyzed by Engineered Cytochrome P450 Enzymes

Pedro S. Coelho,[1]* Eric M. Brustad,[2]* Arvind Kannan,[1] Frances H. Arnold[1]†

Transition metal–catalyzed transfers of carbenes, nitrenes, and oxenes are powerful methods for functionalizing C=C and C–H bonds. Nature has evolved a diverse toolbox for oxene transfers, as exemplified by the myriad monooxygenation reactions catalyzed by cytochrome P450 enzymes. The isoelectronic carbene transfer to olefins, a widely used C–C bond–forming reaction in organic synthesis, has no biological counterpart. Here we report engineered variants of cytochrome $P450_{BM3}$ that catalyze highly diastereo- and enantioselective cyclopropanation of styrenes from diazoester reagents via putative carbene transfer. This work highlights the capacity to adapt existing enzymes for the catalysis of synthetically important reactions not previously observed in nature.

The many strategies for functionalizing C=C and C–H bonds that have evolved in nature have captivated the imaginations of chemists and form the foundation of biomimetic chemistry (*1*, *2*). The reverse of this, using inspiration from synthetic chemistry to discover and develop new biocatalysts, is a nascent frontier in molecular engineering, whose recent highlights include C–H activation by artificial rhodium enzymes (*3*) and the de novo design of Diels-Alderases (*4*). Synthetic chemists have developed powerful methods for direct C=C and C–H functionalization based on transition metal–catalyzed carbenoid and nitrenoid transfers, reactions that are widely used to synthesize natural product intermediates and pharmaceuticals (*5*). The asymmetric cyclopropanation of olefins with high-energy carbene precursors (e.g., acceptor-substituted diazo reagents) is a hallmark reaction that generates up to three stereogenic centers in a single step to make the important cyclopropane motif, featured in many natural products and therapeutic agents (*6*). Limited to using physiologically accessible reagents, nature catalyzes intermolecular cyclopropane formation through wholly different strategies, typically involving olefin addition to the methyl cation of *S*-adenosyl methionine or through cyclization of dimethylallyl pyrophosphate–derived allylic carbenium ions (*7*). As a result, the diverse cyclopropanation products that can be formed by metallocarbene chemistry cannot be readily accessed by engineering natural cyclopropanation enzymes. We hypothesized that a natural metalloenzyme, the iron-heme–containing cytochrome P450, could be engineered to catalyze formal carbenoid transfers, thereby combining the high levels of regio- and stereoselectivity of enzymes with the synthetic versatility of carbene-based strategies.

Members of the cytochrome P450 enzyme family catalyze myriad oxidative transformations, including hydroxylation, epoxidation, oxidative ring coupling, heteroatom release, and heteroatom oxygenation (*8*). Most transformations encompassed by this broad catalytic scope manifest the reactivity of the same high-valent iron-oxene intermediate, compound I (Fig. 1). Inspired by the impressive chemo-, regio-, and stereoselectivities with which cytochrome P450s can insert O atoms into C–H and C=C bonds, we investigated whether these enzymes could be engineered to mimic this chemistry for isoelectronic carbene transfer reactions via a high-valent iron-carbenoid species (Fig. 1). Here we report that variants of the cytochrome P450 from *Bacillus megaterium* (CYP102A1, or $P450_{BM3}$) are efficient catalysts for the asymmetric metallocarbene-mediated cyclopropanation of styrenes.

Because iron porphyrins catalyze carbene-based cyclopropanations (*9*, *10*), we first probed whether some common heme proteins display measurable levels of cyclopropanation activity in aqueous media (phosphate buffer, with 5% methanol cosolvent). We chose the reaction between styrene and ethyl diazoacetate (EDA) (Fig. 2), a well-recognized model system for validating new cyclopropanation catalysts. Initial experiments showed that optimal formation of the desired cyclopropanation products occurred in the presence of a reducing agent (e.g., sodium dithionite, $Na_2S_2O_4$) under anaerobic conditions (tables S1 to S4). Horseradish peroxidase (HRP), cytochrome c (cyt c), myoglobin (Mb), and $P450_{BM3}$ all displayed multiple turnovers toward the cyclopropane products, with HRP, cyt c, and Mb showing negligible enantioinduction, and formed the trans cyclopropane with over 90% diastereoselectivity, which is comparable to the diastereoselectivity induced by free hemin (table S1). $P450_{BM3}$, despite forming the cyclopropane products in low yield, catalyzed the reaction with different diasteroselectivity (cis:trans 37:63) and slight enantioinduction (Table 1), showing that carbene transfer and selectivity are dictated by the heme cofactor bound in the enzyme active site.

We then explored whether the activity and selectivity of heme-catalyzed cyclopropanation could be enhanced by engineering the protein sequence. $P450_{BM3}$ is a well-studied, soluble, self-sufficient (heme and diflavin reductase domains are fused in a single polypeptide, ~120 kD), long-chain, fatty acid monooxygenase. More than a decade of protein engineering attests to the functional plasticity of this biocatalyst (*11*). From our work using directed evolution to engineer cytochrome $P450_{BM3}$ for synthetic applications, we have accumulated thousands of variants that exhibit monooxygenase activity on a wide range of substrates (*12*). We tested some of these variants

[1]Division of Chemistry and Chemical Engineering, California Institute of Technology, Pasadena, CA 91125, USA. [2]Department of Chemistry and Carolina Center for Genome Sciences, University of North Carolina at Chapel Hill, Chapel Hill, NC 27599, USA.

*These authors contributed equally to this work.
†To whom correspondence should be addressed. E-mail: frances@cheme.caltech.edu

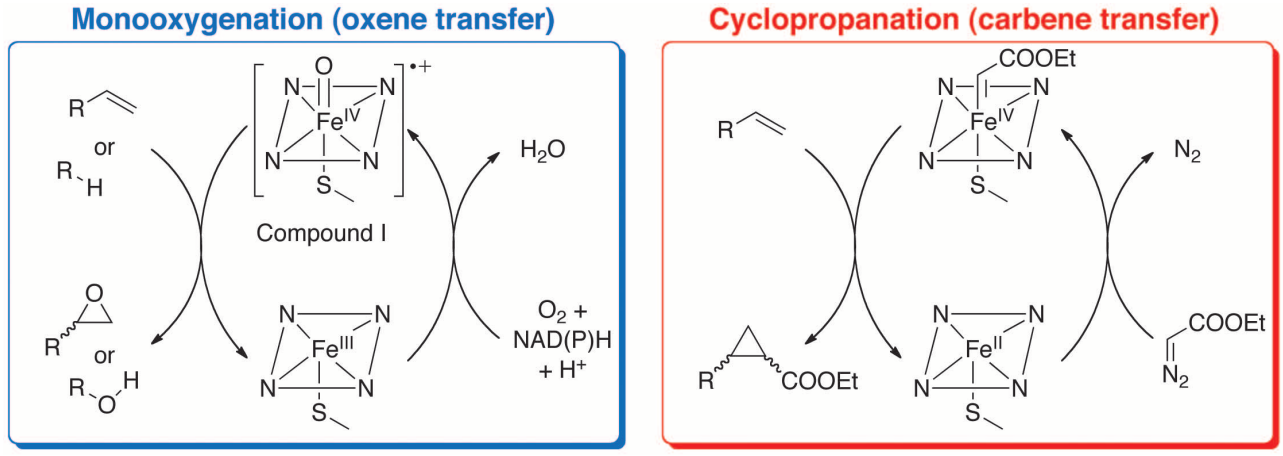

Fig. 1. (**Left**) Canonical mode of reactivity of cytochrome P450s. Monooxygenation of olefins and C-H bonds to epoxides and alcohols catalyzed by the ferryl porphyrin radical intermediate (compound I). (**Right**) Artificial mode of formal carbene transfer activity of cytochrome P450s, using diazoester reagents as carbene precursors.

for altered cyclopropanation diastero- and enantioselectivity by analysis of product distributions using gas chromatography (GC) with a chiral stationary phase. A panel of 92 $P450_{BM3}$ variants, chosen for diversity of activity and protein sequence, was screened in *Escherichia coli* lysate for the reaction of styrene and EDA under aerobic conditions in the presence of $Na_2S_2O_4$ (tables S5 and S6). The 10 most promising hits were selected for purification and characterization under standardized anaerobic reaction conditions (Table 1 and table S7).

Five of the 10 selected P450s showed improvements in activity as compared to the wild type [total turnover numbers (TTNs) > 100], a comprehensive range of diastereoselectivities, with cis:trans ratios varying from 9:91 to 60:40, and up to 95% enantioselectivities (table S7). For example, variant H2-5-F10, which contains 16 amino acid substitutions, catalyzes 294 total turnovers, equivalent to ~58% yield under these conditions (0.2% enzyme loading with respect to EDA). This represents a 50-fold improvement over wild-type $P450_{BM3}$. Furthermore, mutations affect both the diastereo- and enantioselectivity of cyclopropanation: H2-5-F10 favors the trans cyclopropanation product (cis:trans 16:84) with 63% enantiomeric excess (ee_{trans}), whereas H2A10, with a TTN of 167, shows reversed diastereoselectivity (cis:trans 60:40) with high enantioselectivity (95% ee_{cis}).

We used H2A10 to verify the role of the enzyme in catalysis and identify optimal conditions (table S8 and figs. S1 and S2). Heat inactivation produced diastereo- and enantioselectivities similar to those obtained with free hemin, consistent with protein denaturation and release of the cofactor. Complete inhibition was achieved by preincubating the reaction mixture with carbon monoxide, which irreversibly binds the reduced P450 heme, confirming that catalysis occurs at the active site. Air inhibited the cyclopropanation reaction by about 50%, showing that dioxygen and EDA compete for reduced Fe^{II}. Cyclopropanation was also achieved with NADPH (reduced nicotinamide adenine dinucleotide phosphate) as the reductant, confirming that the activity can also be driven by the endogenous electron transport machinery of the diflavin-containing reductase domain. The presence of a reducing agent in substoichiometric amounts proved essential for cyclopropanation (table S9), implying that the active species is Fe^{II} rather than the resting-state Fe^{III}.

Fig. 2. Absolute stereoselectivity of select $P450_{BM3}$ cyclopropanation catalysts. Reaction conditions were as follows: 20 μM catalyst, 30 mM styrene, 10 mM EDA, 10 mM $Na_2S_2O_4$, under argon in aqueous potassium phosphate buffer (pH 8.0) and 5% MeOH cosolvent for 2 hours at 298 K. Enzyme loading was 0.2 mol % with respect to EDA. The structures of each product stereoisomer are shown above the reaction gas chromatograms.

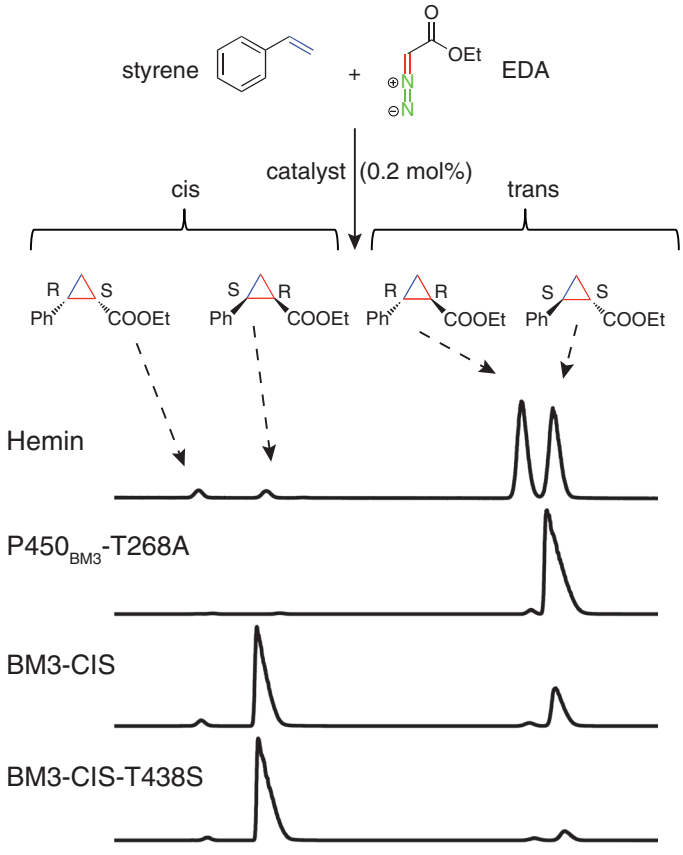

Highly active $P450_{BM3}$ variants H2A10, H2-5-F10, and H2-4-D4 have three to five active-site alanine substitutions with respect to 9-10A-TS-F87V (12 mutations from $P450_{BM3}$, supplementary materials text), which itself shows negligible cyclopropanation activity. These variants exhibit a range of TTNs, diastereoselectivity, and enantioselectivity (Table 1). To better understand how protein sequence controls P450-mediated cyclopropanation, we constructed 12 variants to

Table 1. Stereoselective $P450_{BM3}$ cyclopropanation catalysts. Reactions were run in aqueous phosphate buffer (pH 8.0) and 5% MeOH cosolvent at room temperature under argon with 30 mM styrene, 10 mM EDA, 0.2 mol % catalyst (with respect to EDA), and 10 mM $Na_2S_2O_4$. Yields, diastereomeric ratios, and enantiomeric excess were determined by GC analysis. Yields are based on EDA. See the supplementary text for protein sequences indicating mutations from wild-type $P450_{BM3}$.

Catalyst	% yield	TTN	cis:trans	% ee_{cis}*	% ee_{trans}†
Hemin	15	73	6:94	–1	0
$P450_{BM3}$	1	5	37:63	–27	–2
$P450_{BM3}$-T268A	65	323	1:99	–15	–96
9-10A-TS-F87V	1	7	35:65	–41	–8
H2-5-F10	59	294	16:84	–41	–63
H2A10	33	167	60:40	–95	–78
H2-4-D4	41	206	53:47	–79	–33
BM3-CIS	40	199	71:29	–94	–91
BM3-CIS-I263A	38	190	19:81	–62	–91
BM3-CIS-A328G	37	186	83:17	52	–45
BM3-CIS-T438S	59	293	92:8	–97	–66

*(*R*,*S*) – (*S*,*R*). †(*R*,*R*) – (*S*,*S*).

Table 2. Scope of P450-catalyzed cyclopropanation of styrenyl substrates. Ar = *p*-X-C_6H_4. Reaction conditions were as follows: 20 μM catalyst, 30 mM olefin, 10 mM diazoester, 10 mM $Na_2S_2O_4$, under argon in aqueous potassium phosphate buffer (pH 8.0) and 5% MeOH cosolvent for 2 hours at 298 K. Enzyme loading was 0.2 mol % with respect to diazoester. N/A, not available when enantiomers did not separate to baseline resolution.

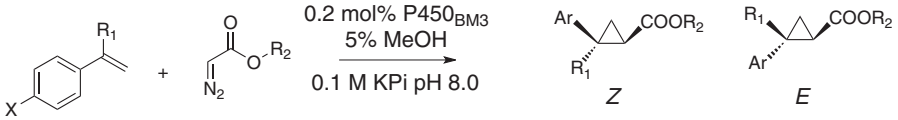

Reagents	P450 catalyst	TTN	*Z* : *E*	%ee_Z	%ee_E
R_1 = H, X= Me, R_2 = Et	BM3-CIS	228	78 : 22	-81	N/A
R_1 = H, X= OMe, R_2 = Et	H2-5-F10	364	11 : 89	38	N/A
R_1 = H, X= CF_3, R_2 = Et	7-11D	120	76 : 24	31	59
R_1 = Me, X= H, R_2 = Et	7-11D	157	41 : 49	42	N/A
R_1 = H, X= H, R_2 = *t*-Bu	H2A10	120	3 : 97	N/A	N/A

assess the contributions of individual alanines to catalysis and stability [table S10 (*13*)]. T268A is key for achieving high cyclopropanation activity, and this mutation alone converts inactive 9-10A-TS-F87V into an active cyclopropanation catalyst. Variant 9-10A-TS-F87V-T268A (here called BM3-CIS) is a competent cyclopropanation catalyst (199 TTNs), displays strong preference for the cis product (cis:trans 71:29), forms both diastereomers with over 90% *ee,* and is as stable as wild-type $P450_{BM3}$. Other active site alanine mutations tune the product distribution. The addition of I263A to BM3-CIS reverses diastereoselectivity (cis:trans 19:81). We also investigated the effects of similar mutations introduced in the poorly active wild-type $P450_{BM3}$ (table S11). $P450_{BM3}$-T268A, with a single mutation, is an active cyclopropanation catalyst (323 TTNs, Table 1) with exquisite trans-selectivity (cis:trans 1:99) and high enantioselectivity for the major diastereomer (–96% ee_{trans}, Fig. 1). Whereas BM3-CIS is a cis-selective cyclopropanation catalyst, identical active-site mutations in wild-type $P450_{BM3}$ result in a trans-selective enzyme (table S11), demonstrating that mutations outside of the active site also influence the stereochemical outcome.

Because the design of cis-selective small-molecule catalysts for diazocarbonyl-mediated cyclopropanations has proven more challenging than that of their trans counterparts (*14*), we investigated whether active-site engineering of $P450_{BM3}$ could provide robust cis-selective water-compatible catalysts to complement existing organometallic systems (*15*). We chose five active site residues (L181, I263, A328, L437, and T438) for individual site-saturation mutagenesis (*13*). The A328G, T438A, T438S, and T438P variants exhibited enhanced cis-selectivity (table S12). A328G also reversed the enantioselectivity for the cis-diastereomer (Table 1). BM3-CIS-T438S displayed the highest diastereo- and enantioselectivities (cis:trans 92:8 and –97% ee_{cis}) and maintained TTNs comparable to those of BM3-CIS (Table 1).

BM3-CIS exhibits Michaelis-Menten kinetics (fig. S3 and table S13) with relatively high Michaelis constant values for the olefin (~1.5 mM) and the diazoester (~5 mM), reflecting the lack of evolutionary pressure for this enzyme to bind these substrates. BM3-CIS exhibits a notable catalytic rate constant (k_{cat}) for cyclopropanation of 100 min^{-1}, comparable to the k_{cat} of many native P450s for hydroxylation, but about 50 times less than $P450_{BM3}$-catalyzed fatty acid hydroxylation (table S14). Free hemin does not exhibit saturation kinetics and displays slower initial rates than BM3-CIS (only 30 min^{-1} at 10 mM styrene and 15 mM EDA), indicating that the protein scaffold enhances k_{cat} as compared to the free cofactor in solution. When used at 0.2 mole % (mol %) equivalent, BM3-CIS–catalyzed cyclopropanations reached completion after 30 min. Adding more EDA enhanced turnovers for cyclopropanes and preserved BM3-CIS stereoselectivity (table S15), confirming catalyst integrity and implying that the reaction stops because of EDA depletion rather than inactivation.

To assess the substrate scope of $P450_{BM3}$-catalyzed cyclopropanation, we investigated the activities of six variants against a panel of olefins and diazo compounds (Table 2 and tables S16 to S20). P450 cyclopropanation is robust to both electron-donating (*p*-vinylanisole and *p*-vinyltoluene) and electron-withdrawing (*p*-trifluoromethylstyrene) substitutions on styrene, and variant 7-11D showed consistent cis-selectivity for these substrates. The P450s were also active on 1,1-disubstituted olefins (i.e., α-methyl styrene), with chimeric P450 C2G9R1 forming cyclopropanes in 77% yield (with respect to EDA). The P450s were only moderately active with *t*-butyl diazoacetate as substrate (<30% yield), forming the trans product with >87% selectivity and offering no advantage over free hemin (table S20). For reactions involving EDA and aryl-substituted olefins, however, the P450s consistently outperformed the free cofactor in both activity and stereoselectivity.

Screening natural enzymes against synthetic reagents chosen based on chemical intuition offers a simple strategy for identifying enzymes with basal levels of non-native activity. As we have shown, a single mutation can be enough to promote such activity and achieve synthetically useful stereoselectivities. The accumulation of beneficial mutations by directed evolution or other protein engineering strategies can generate a spectrum of highly active catalysts for desired substrate and product specificities. The established reaction promiscuity of natural enzymes (*16*, *17*) and the

surprising ease with which cyclopropanation activity could be installed into $P450_{BM3}$ suggest that this approach will be useful for other synthetically important transformations for which biological counterparts do not yet exist.

References and Notes

1. J. T. Groves, *Proc. Natl. Acad. Sci. U.S.A.* **100**, 3569 (2003).
2. R. Breslow, *J. Biol. Chem.* **284**, 1337 (2009).
3. T. K. Hyster, L. Knörr, T. R. Ward, T. Rovis, *Science* **338**, 500 (2012).
4. J. B. Siegel *et al.*, *Science* **329**, 309 (2010).
5. H. M. L. Davies, J. R. Manning, *Nature* **451**, 417 (2008).
6. H. Lebel, J.-F. Marcoux, C. Molinaro, A. B. Charette, *Chem. Rev.* **103**, 977 (2003).
7. L. A. Wessjohann, W. Brandt, T. Thiemann, *Chem. Rev.* **103**, 1625 (2003).
8. E. M. Isin, F. P. Guengerich, *Biochim. Biophys. Acta Gen. Subj.* **1770**, 314 (2007).
9. J. R. Wolf, C. G. Hamaker, J.-P. Djukic, T. Kodadek, L. K. Woo, *J. Am. Chem. Soc.* **117**, 9194 (1995).
10. B. Morandi, E. M. Carreira, *Science* **335**, 1471 (2012).
11. C. J. C. Whitehouse, S. G. Bell, L.-L. Wong, *Chem. Soc. Rev.* **41**, 1218 (2012).
12. J. C. Lewis, F. H. Arnold, *Chimia (Aarau)* **63**, 309 (2009).
13. Materials and methods are available as supplementary materials on *Science* Online.
14. A. Caballero, A. Prieto, M. M. Diaz-Requejo, P. J. Perez, *Eur. J. Inorg. Chem.* **2009**, 1137 (2009).
15. I. Nicolas, P. Le Maux, G. Simonneaux, *Coord. Chem. Rev.* **252**, 727 (2008).
16. U. T. Bornscheuer, R. J. Kazlauskas, *Angew. Chem. Int. Ed.* **43**, 6032 (2004).
17. O. Khersonsky, C. Roodveldt, D. S. Tawfik, *Curr. Opin. Chem. Biol.* **10**, 498 (2006).

Acknowledgments: This work was funded by the Division of Chemical Sciences, Geosciences, and Biosciences, Office of Basic Energy Sciences of the U.S. Department of Energy through grant DE-FG02-06ER15762. E.M.B. was supported by a Ruth M. Kirschstein National Institutes of Health (NIH) postdoctoral fellowship, award number F32GM087102, from the National Institute of General Medical Sciences and a generous startup fund from the University of North Carolina Chapel Hill. P.S.C., E.M.B., and F.H.A. have filed through the California Institute of Technology a provisional patent application that is based on the results presented here. The authors thank Z. J. Wang for helpful discussions during the preparation of the manuscript.

Supplementary Materials

www.sciencemag.org/cgi/content/full/science.1231434/DC1
Materials and Methods
Supplementary Text
Figs. S1 to S3
Tables S1 to S20
References (*18*–*35*)

12 October 2012; accepted 30 November 2012
Published online 20 December 2012;
10.1126/science.1231434

Metamaterial Apertures for Computational Imaging

John Hunt,[1,4]* Tom Driscoll,[1,2,4] Alex Mrozack,[3] Guy Lipworth,[1,4] Matthew Reynolds,[4] David Brady,[4] David R. Smith[1,4]

By leveraging metamaterials and compressive imaging, a low-profile aperture capable of microwave imaging without lenses, moving parts, or phase shifters is demonstrated. This designer aperture allows image compression to be performed on the physical hardware layer rather than in the postprocessing stage, thus averting the detector, storage, and transmission costs associated with full diffraction-limited sampling of a scene. A guided-wave metamaterial aperture is used to perform compressive image reconstruction at 10 frames per second of two-dimensional (range and angle) sparse still and video scenes at K-band (18 to 26 gigahertz) frequencies, using frequency diversity to avoid mechanical scanning. Image acquisition is accomplished with a 40:1 compression ratio.

Imaging systems can be characterized by object dimension [for instance, two-dimensional (2D) for photographs] and information dimension (for example, the number of pixels in an image). Conventional imaging systems are built around the assumption that the object dimension must be conserved in the information dimension, regardless of the inherent information content of the scene. Compressive measurement leverages the realization that measurements need not conserve form of dimension in this sense (*1*–*3*). Indeed, the concept of dimension indicates that measurements are well ordered in some space, implying that adjacent measurements sample similar object data. Information-transfer efficiency, however, is maximized if object data measured by successive measurements are as distinct as possible.

At the diffraction limit, the finite size of the aperture used to form an image imposes a maximum pixel dimension N equal to the space-bandwidth product (SBP), which represents the number of measurement modes needed to exactly reproduce an arbitrary scene (*4*, *5*). In a conventional imaging system, the measurement modes might be thought of as diffraction-limited spots, each of which samples a small portion of the scene (Fig. 1A). Because these modes have little or no spatial overlap in the detector plane, they can be acquired nearly independently and simultaneously with N detectors, such as a charge-coupled device array. However, for natural scenes, many of the modes provide little to no useful data; therefore, they can be substantially compressed without excessive loss of image fidelity (*6*).

The concept of a measurement mode can be generalized, such that the imaging process can be expressed mathematically by the relation $\mathbf{g} = \mathbf{H}\mathbf{f}$, where $\mathbf{g}$ is a collection of measurements, $\mathbf{H}$ is the measurement matrix (a row-wise array of all measurement modes), and $\mathbf{f}$ is the sampled scene. To form a completely determined data set of measurements (thus enabling a unique linear solution for $\mathbf{f}$), the rank of $\mathbf{H}$ must equal the scene's data dimension (*7*). Compressive sampling allows reconstruction of underdetermined scenes, finding $\mathbf{f}$ by solving the minimization problem $\arg\min_{\mathbf{f}} \|\mathbf{g} - \mathbf{H}\mathbf{f}\|_2^2 + \lambda R(\mathbf{f})$, where $\arg\min_{\mathbf{f}}$ denotes the value of $\mathbf{f}$ that minimizes the expression, λ is a scalar weighting factor, and $R(\mathbf{f})$ expresses some prior knowledge about the likely composition of the scene. Typically in compressive sampling, R is the l_1-norm of the scene, represented in an appropriate basis, which reflects the inherent sparsity that exists in natural scenes. This nonlinear minimization problem is rigorously solvable, even with highly underdetermined measurement data sets (*8*–*10*).

Imaging systems for radio frequency and millimeter-wave electromagnetics have generally been of two types: scanned single-pixel systems and multielement phased-arrays (or synthetic phased arrays). The measurement modes used by classical single-pixel systems are typically inefficient at collecting imaging data. For instance, a rasterizing scanned beam collects information about only one point in space at a time. Multielement phased array systems have much more flexibility in the measurement modes they can access, but these systems sacrifice the size, weight, power, and price advantages of single-pixel systems.

New approaches to imaging at these frequencies have made use of lenses and spatially modulated masks combined with single-pixel detectors to make compressed measurements. One of the pioneering implementations of this form of compressive imaging, depicted in Fig. 1B, was carried out at optical (*11*) and terahertz frequencies with the use of random static (*12*) and dynamic (*13*) masks. Other groups have presented additional ways to introduce mode diversity (*14*). We show that metamaterial apertures have distinct advantages for compressive imaging because they can be engineered to support custom-designed complex measurement modes that vary with frequency. Leveraging the same electromagnetic

[1]Center for Metamaterials and Integrated Plasmonics, Duke University, Box 90291, Durham, NC 27708, USA. [2]Department of Physics, University of California San Diego, La Jolla, CA 92093, USA. [3]Fitzpatrick Institute for Photonics and Electrical and Computer Engineering, Duke University, Durham, NC 27708, USA. [4]Department of Electrical and Computer Engineering, Duke University, Durham, NC 27708, USA.

*To whom correspondence should be addressed. E-mail: john.hunt@duke.edu

Olefin Cyclopropanation via Carbene Transfer Catalyzed by Engineered Cytochrome P450 Enzymes

Pedro S. Coelho, Eric M. Brustad, Arvind Kannan and Frances H. Arnold

Science **339** (6117), 307-310.
DOI: 10.1126/science.1231434originally published online December 20, 2012

Putting a C in Cytochrome

Cytochrome P450 enzymes oxidize hydrocarbons using a highly reactive iron oxo intermediate. Much research has focused on tuning the protein structure to broaden the range of hydrocarbons that can be functionalized. **Coelho *et al.*** (p. 307, published online 20 December; see the Perspective by **Narayan and Sherman**) substituted a carbene source for the oxygen to make a P450 mutant a cyclopropanation catalyst whereby a carbon fragment is transferred in place of oxygen. Though carbene activation by iron is chemically analogous to the native oxygen activation pathway, the overall reaction is completely different from any known enzymatic transformation.